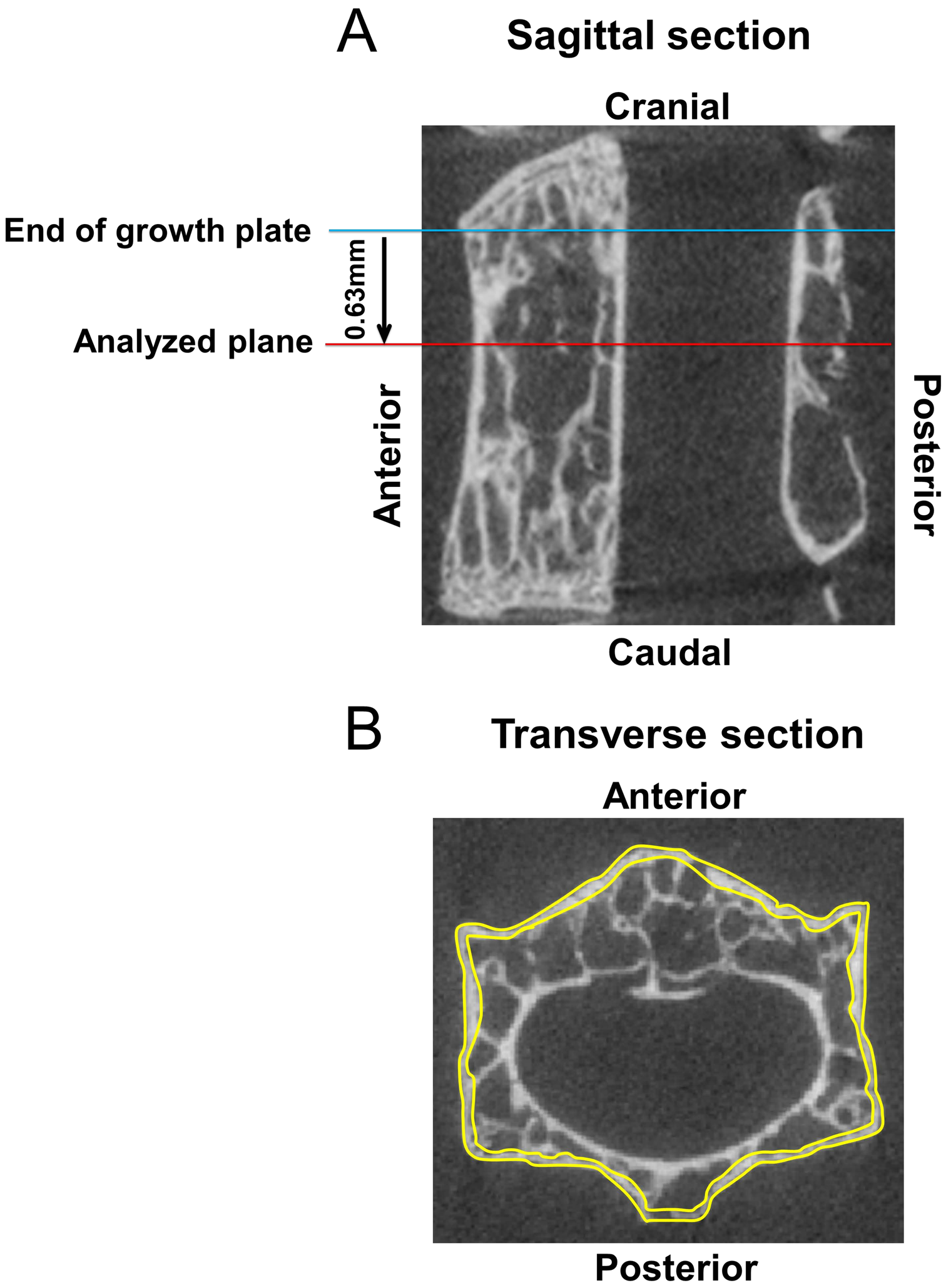

Figure S1. Schematic of the cortical bone area analysis of third lumbar vertebra. (A) Sagittal section of vertebra. The plane (red line) used for the analysis of cortical bone area was established 0.63mm inferior to the end of the cranial growth plate (blue line). (B) Transverse section of vertebra at indicated plane in (A). The area between two yellow lines indicates the analyzed cortical bone area.

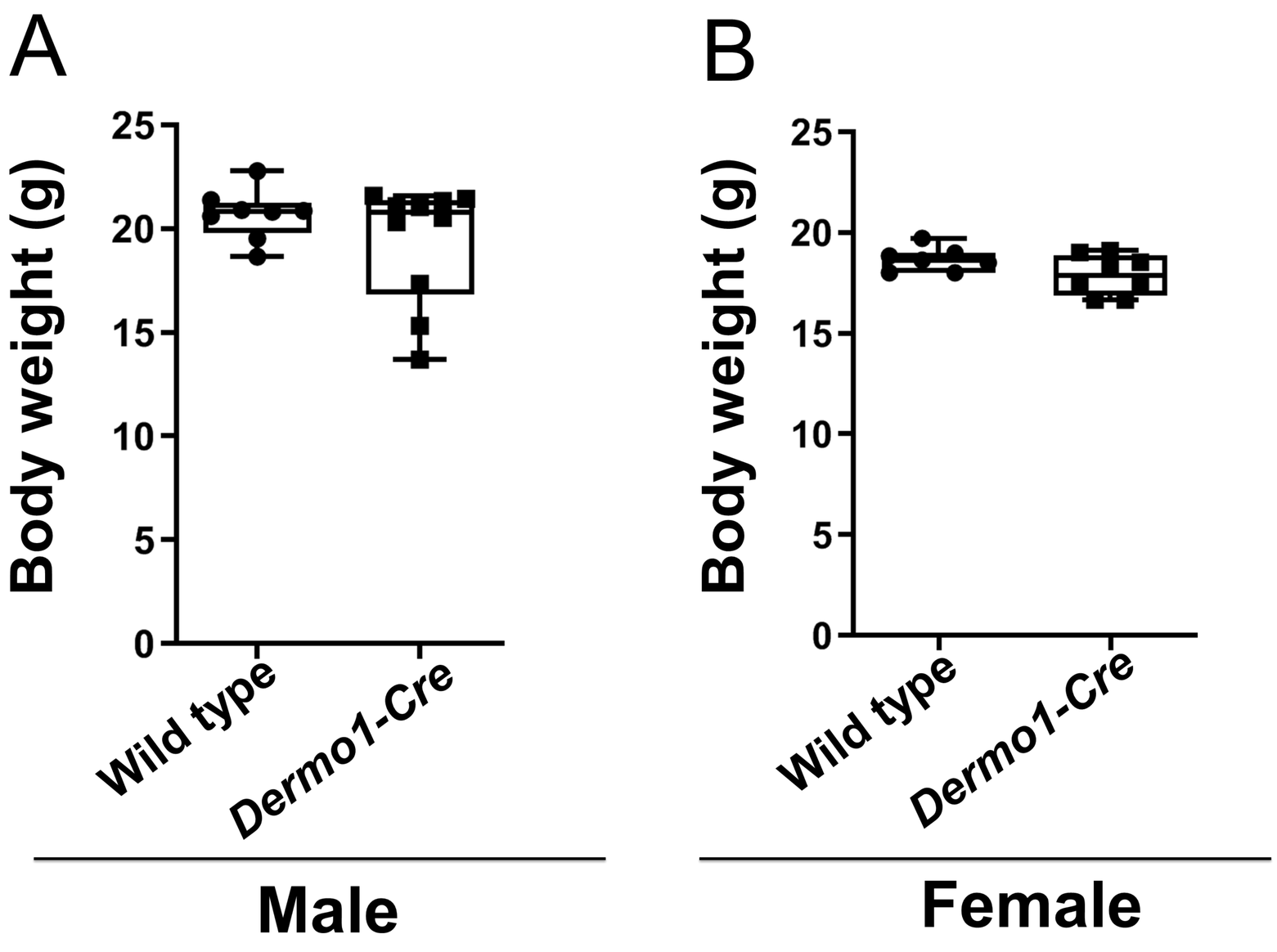

Figure S2. Body weight of 2-month-old wild type and *Dermo1-Cre* mice. (A) Male mice (n=8 for wild type group and n=10 for *Dermo1-Cre* group). (B) Female mice (n=7 for wild type group and n=8 for *Dermo1-Cre* group). Values were presented as median and interquartile range.

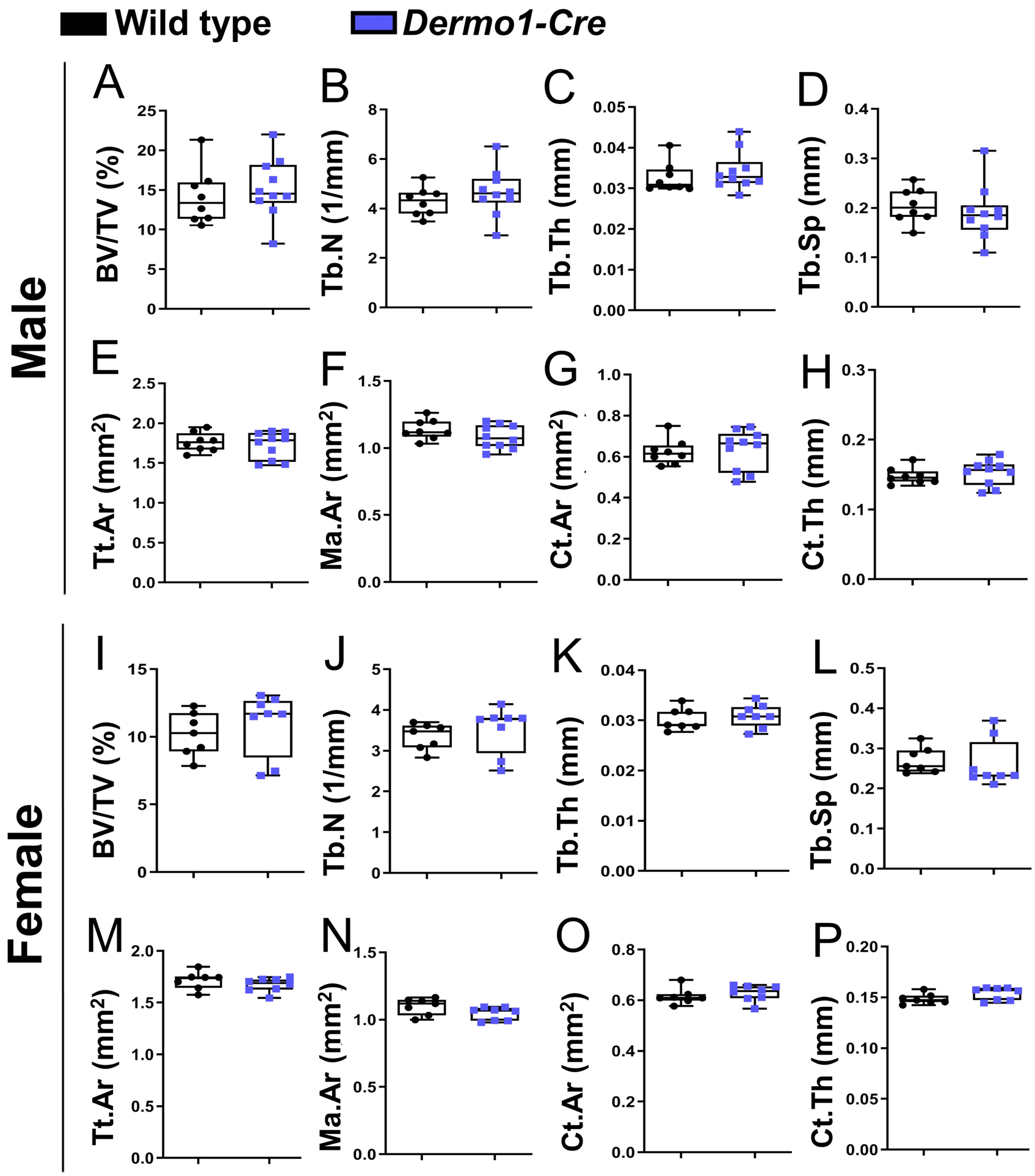

Figure S3. *Dermo1-Cre* does not affect bone development. MicroCT analysis of 2-month-old wild type and *Dermo1-Cre* mice in femoral cortical and trabecular bone. (A-H) Male mice (n=8 for wild type group and n=10 for *Dermo1-Cre* group): (A) BV/TV, bone volume fraction; (B) Tb.N, trabecular number; (C) Tb.Th, trabecular thickness; (D) Tb.Sp, trabecular spacing; (E) Tt.Ar, total cross-sectional area inside the periosteal envelope; (F) Ma.Ar, marrow area; (G) Ct.Ar, cortical bone area; (H) Ct.Th, average cortical thickness. (I-P) Female mice (n=7 for wild type group and n=8 for *Dermo1-Cre* group): (I) BV/TV, bone volume fraction; (J) Tb.N, trabecular number; (K) Tb.Th, trabecular thickness; (L) Tb.Sp, trabecular spacing; (M) Tt.Ar, total cross-sectional area inside the periosteal envelope ; (N) Ma.Ar, marrow area; (O) Ct.Ar, cortical bone area; (P) Ct.Th, average cortical thickness. Values were presented as median and interquartile range.

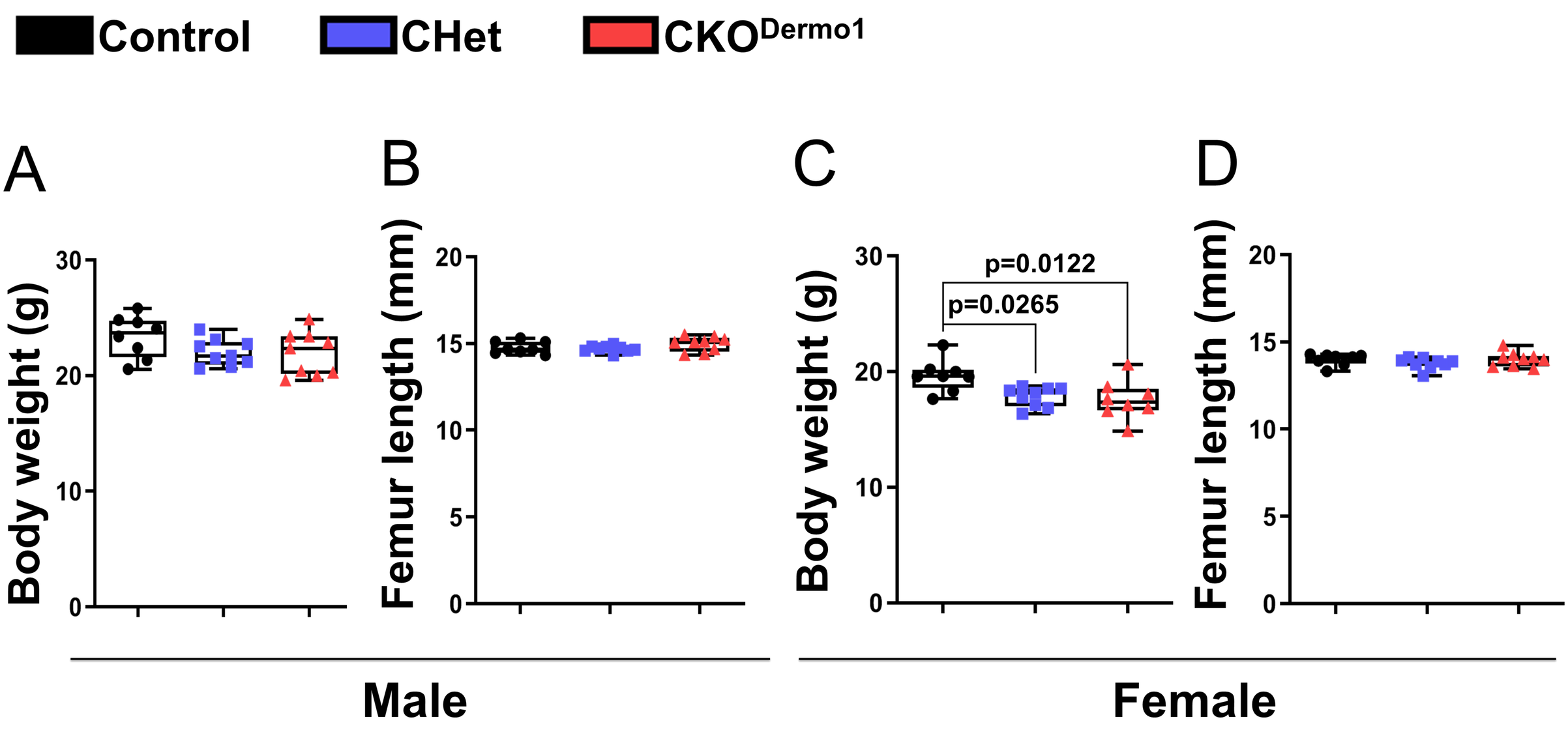

Figure S4. Body weight and femur length of 2-month-old *Fak*$^{flox/flox}$ (Control), *Fak*$^{flox/+}$;*Dermo1-Cre* (CHet) and *Fak*$^{flox/flox}$;*Dermo1-Cre* (CKO^{Dermo1}) mice. (A,B) Body weight (A) and femur length (B) of male mice (n=8 for control group, n=9 for CHet group, and n=9 for CKO^{Dermo1} group). (C,D) Body weight (C) and femur length (D) of female mice (n=8 for control group, n=9 for CHet group, and n=8 for CKO^{Dermo1} group). Values were presented as median and interquartile range.

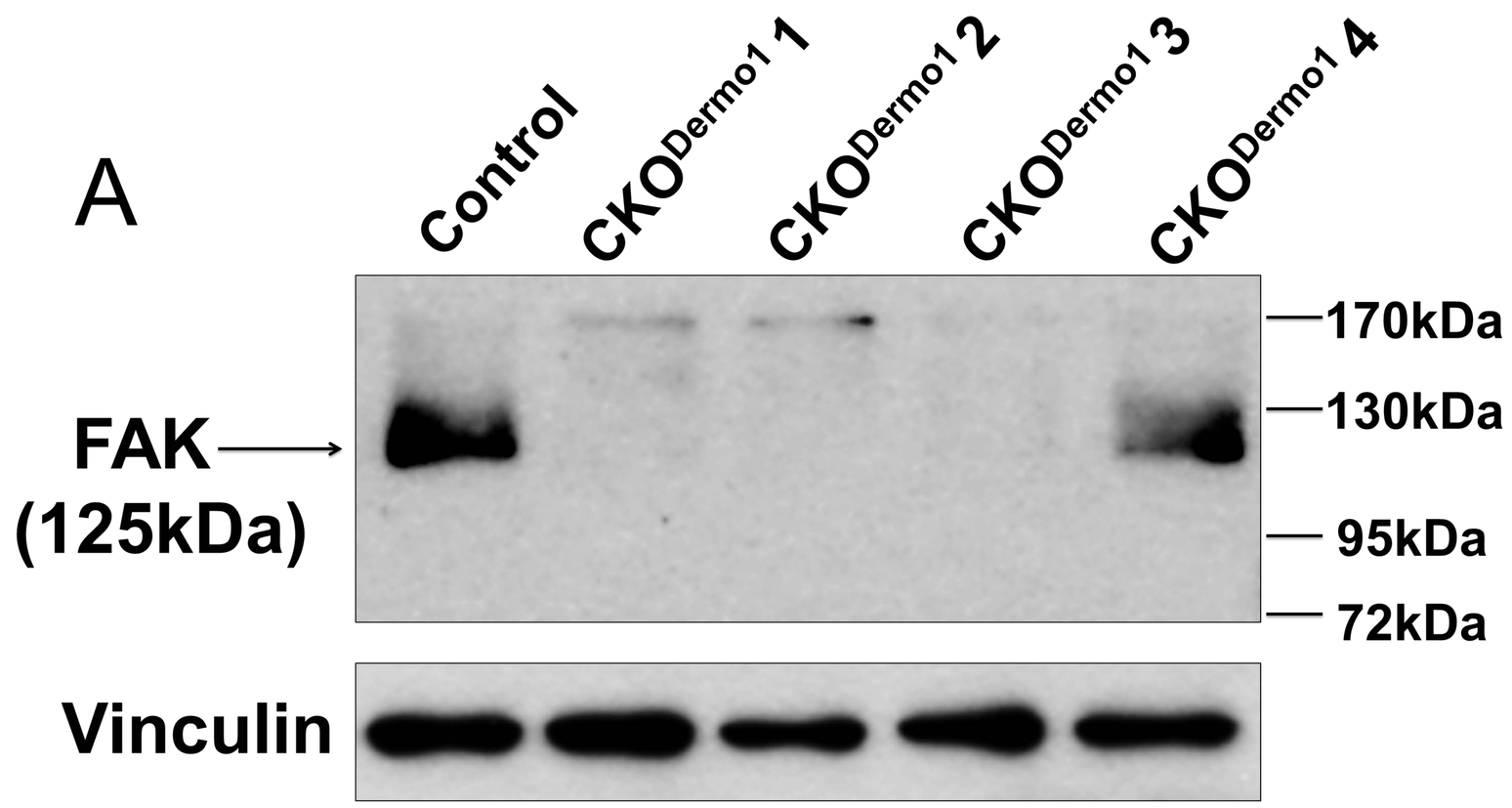

Figure S5. *Fak* deletion efficiency in the femurs of 2-month-old *Fak*$^{flox/flox}$;*Dermo1-Cre* (CKO^{Dermo1}) male and female mice. (A) Representative western blot image showing FAK deletion in femurs isolated from 2-month-old *Fak*$^{flox/flox}$ (Control) and *Fak*$^{flox/flox}$;*Dermo1-Cre* (CKO^{Dermo1}) male mice. Bone marrow were flushed before the protein extraction. (B) Quantification of the relative level of FAK in male mice (n=11 for control group and n=14 for CKO^{Dermo1} group). (C) Quantification of the relative level of FAK in female mice (n=8 per group). Values were presented as median and interquartile range.

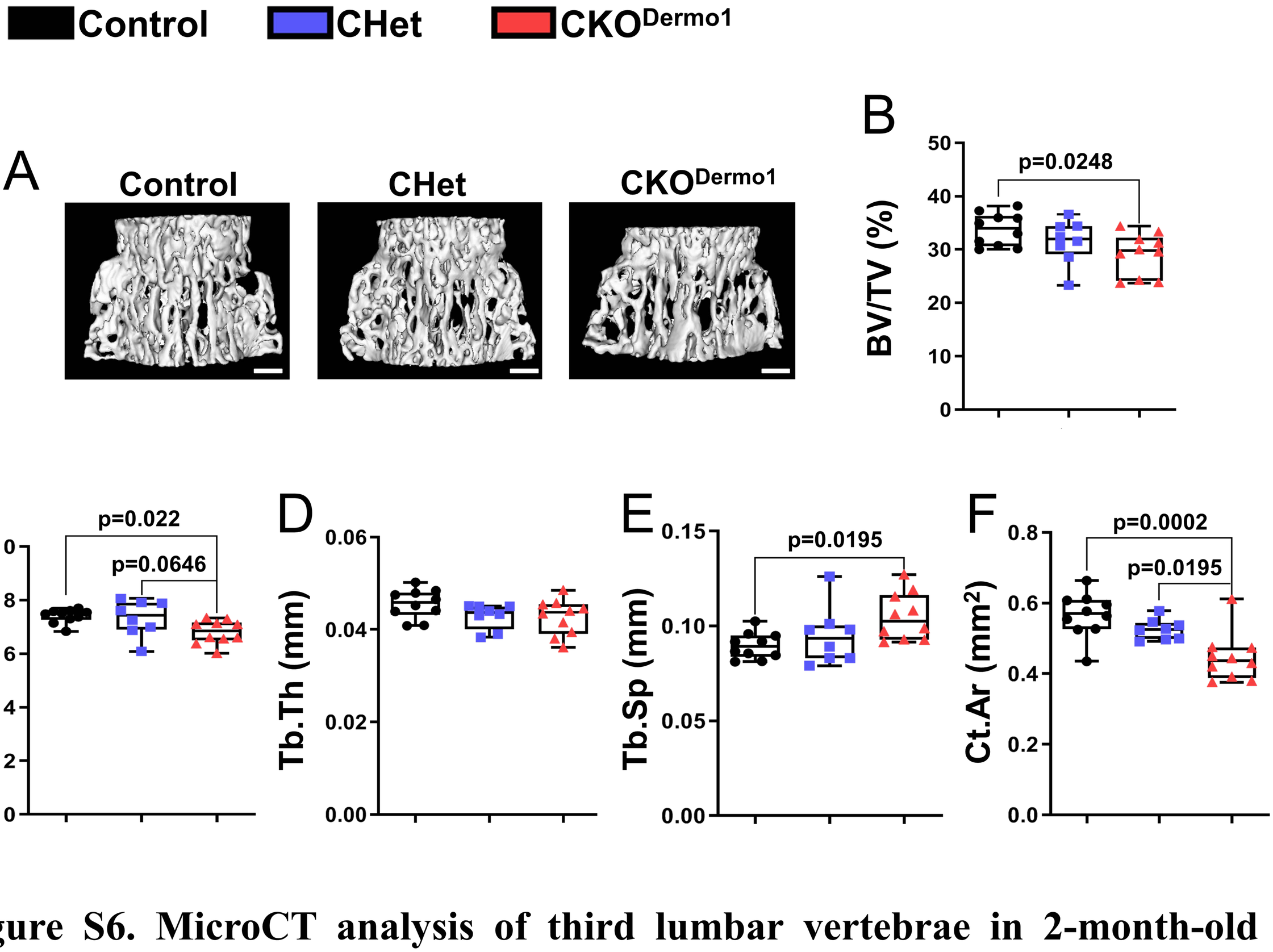

Figure S6. MicroCT analysis of third lumbar vertebrae in 2-month-old *Fak*$^{flox/flox}$ (Control), *Fak*$^{flox/+}$;*Dermo1-Cre* (CHet) and *Fak*$^{flox/flox}$;*Dermo1-Cre* (CKO^{Dermo1}) male mice. (A) Representative microCT image, scale bar=300μm. (B) BV/TV, bone volume fraction. (C) Tb.N, trabecular number. (D) Tb.Th, trabecular thickness. (E) Tb.Sp, trabecular spacing. (F) Cortical bone area of vertebra (n=10 for control group, n=8 for CHet group, and n=10 for CKO^{Dermo1} group). Values were presented as median and interquartile range.

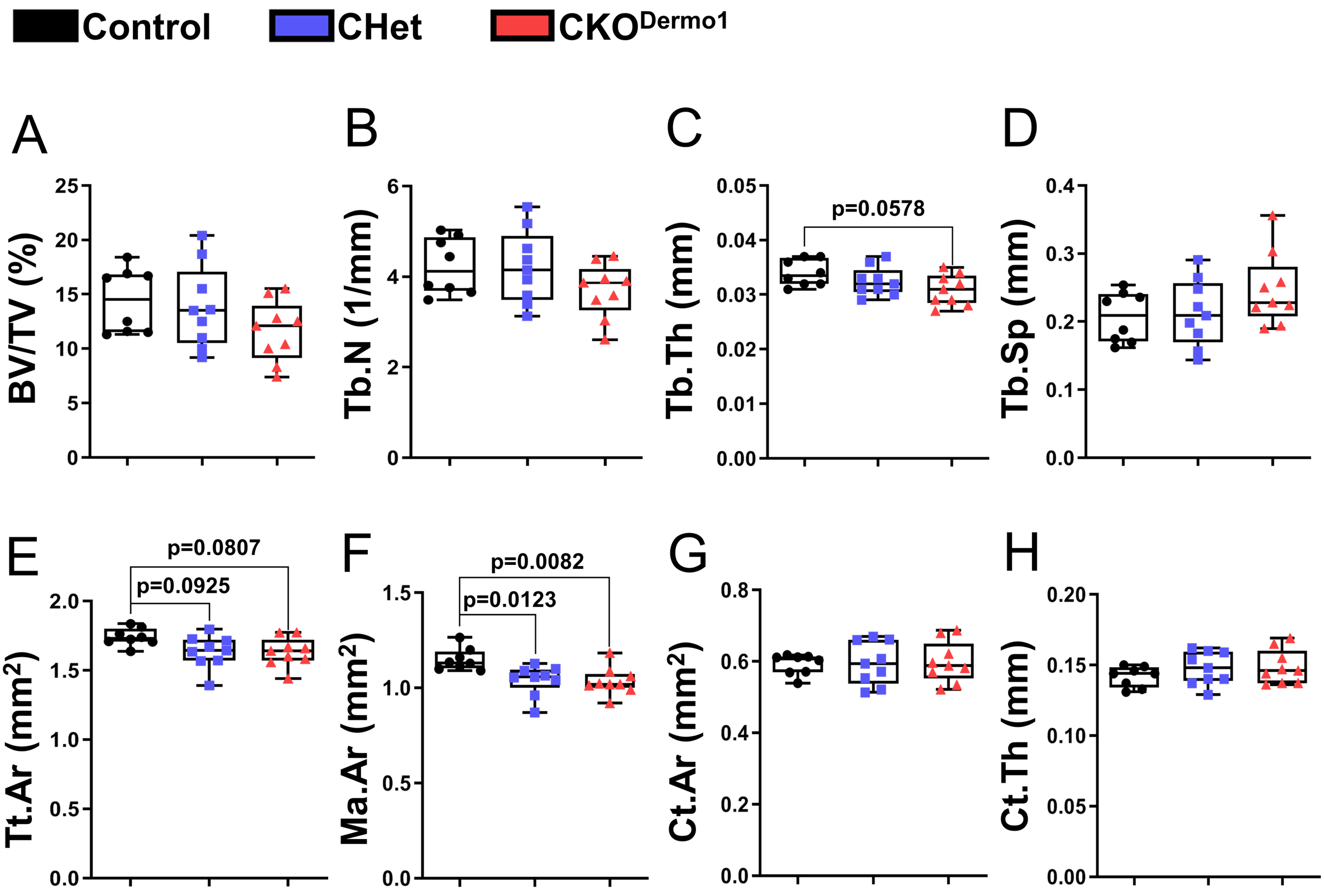

Figure S7. MicroCT analysis of 2-month-old *Fak*$^{flox/flox}$ (Control), *Fak*$^{flox/+}$;*Dermo1-Cre* (CHet) and *Fak*$^{flox/flox}$;*Dermo1-Cre* (CKO^{Dermo1}) female mice. (A) BV/TV, bone volume fraction. (B) Tb.N, trabecular number. (C) Tb.Th, trabecular thickness. (D) Tb.Sp, trabecular spacing. (E) Tt.Ar, total cross-sectional area inside the periosteal envelope. (F) Ma.Ar, marrow area. (G) Ct.Ar, cortical bone area. (H) Ct.Th, average cortical thickness (n=8 for control group, n=9 for CHet group, and n=9 for CKO^{Dermo1} group). Values were presented as median and interquartile range.

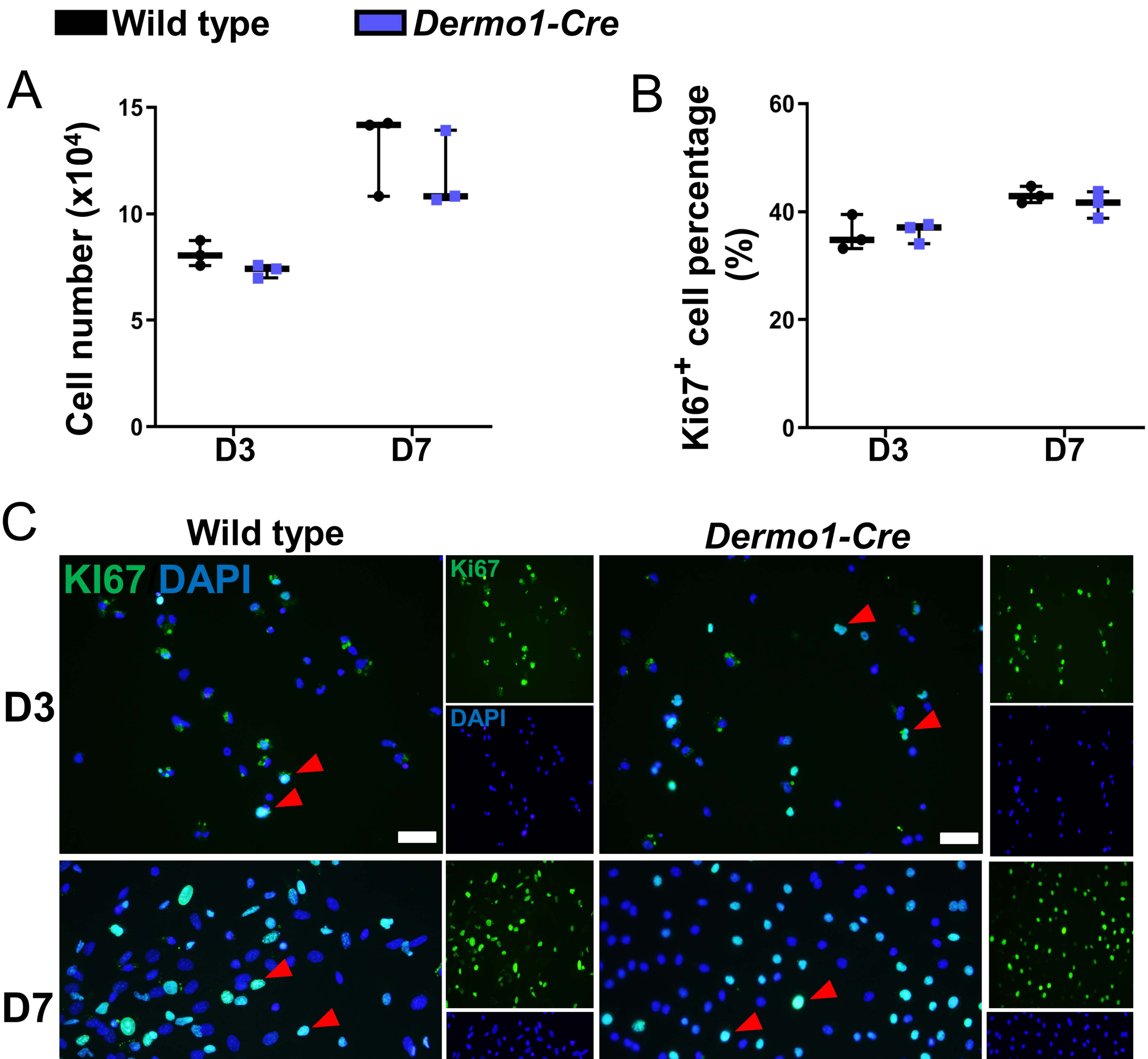

Figure S8. *Dermo1-Cre* does not affect BMSC proliferation. (A) Quantification of cell number cultured for 3 and 7 days (n=3). (B) Quantification of ki67 positive BMSC percentage in the same cultures as (A) (n=3). (C) Representative fluorescent images of Ki67 (green) and Dapi (blue) staining in BMSCs isolated from wild type and *Dermo1-Cre* mice in the cultures described in (B). Red arrow heads point to the $Ki67^{+}DAPI^{+}$cells. Scale bar=20 μm. Values were presented as median and interquartile range.

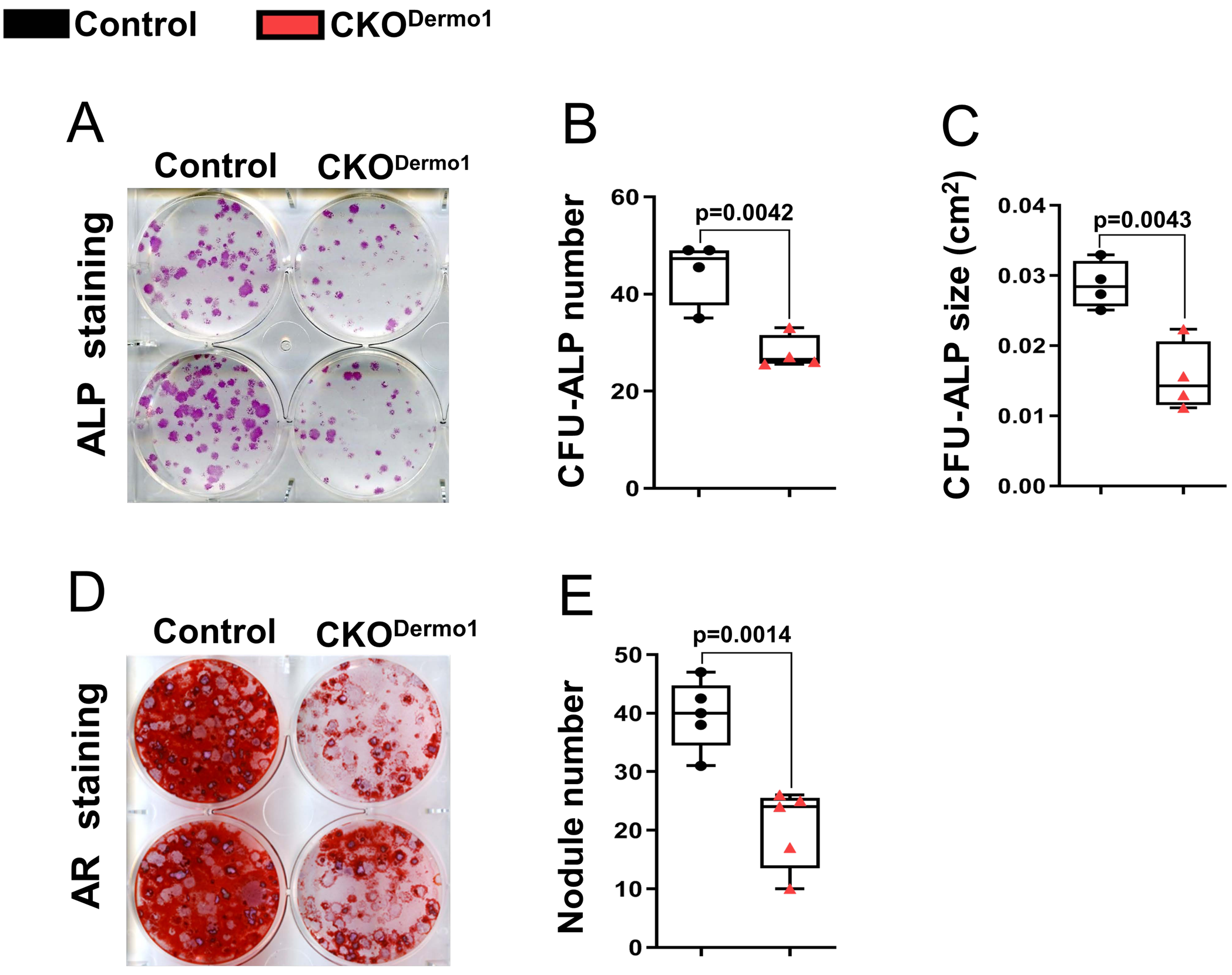

Figure S9. ***Fak*** **deletion in** ***Dermo1*****-expressing cells compromises BMSC osteogenic differentiation.** (A-C) Alkaline phosphatase positive CFU (CFU-ALP) assay of control and CKO^{Dermo1} BMSCs: (A) Representative image of ALP staining at day 10; (B) Quantification of the CFU-ALP number; and (C) Quantification of the CFU-ALP size described in (A). Each data point represents the average of one independent experiment (n=4). (D-E) Mineralization assay of control and CKO^{Dermo1} BMSCs: (D) Representative Alizarin red (AR) staining in control and CKO^{Dermo1} BMSCs at day 21; (E) Quantification of the mineralized nodule number described in (D). Each data point represents the average of one independent experiment (n=5). Values were presented as median and interquartile range.

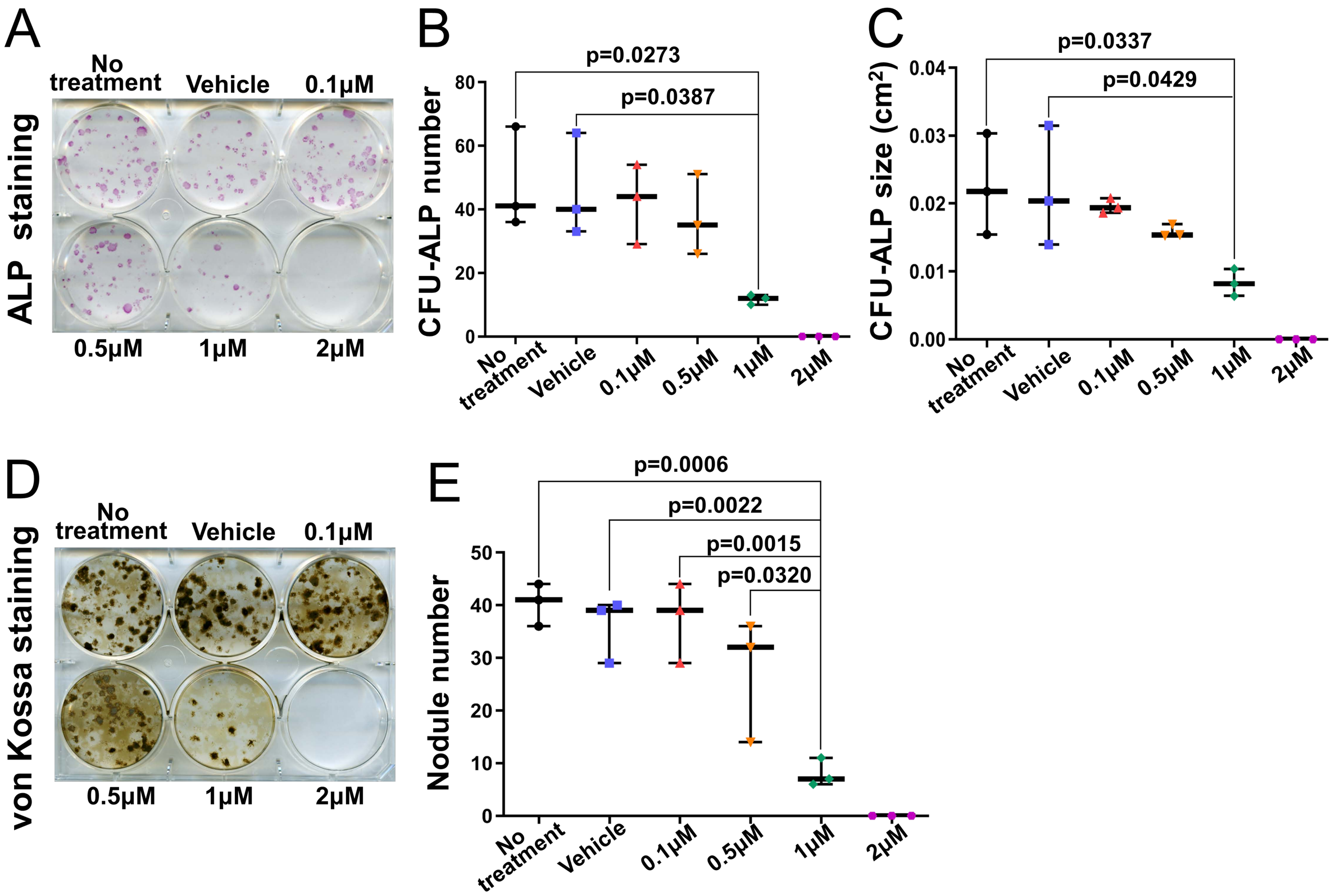

Figure S10. FAK kinase inhibition leads to decreased BMSC differentiation and mineralization. (A) Representative alkaline phosphatase (ALP) staining in BMSCs cultured with indicated doses of FAK inhibitor PF-573,228 for 10 days. (B) Quantification of the CFU-ALP number; and (C) Quantification of the CFU-ALP size described in (A). Each data point represents the average of one independent experiment (n=3). (D) Representative image of von Kossa staining in BMSCs cultured with indicated doses of FAK inhibitor for 21 days. (E) Quantification of the mineralized nodule number described in (D). Each data point represents the average of one independent experiment (n=3). Values were presented as median and interquartile range.

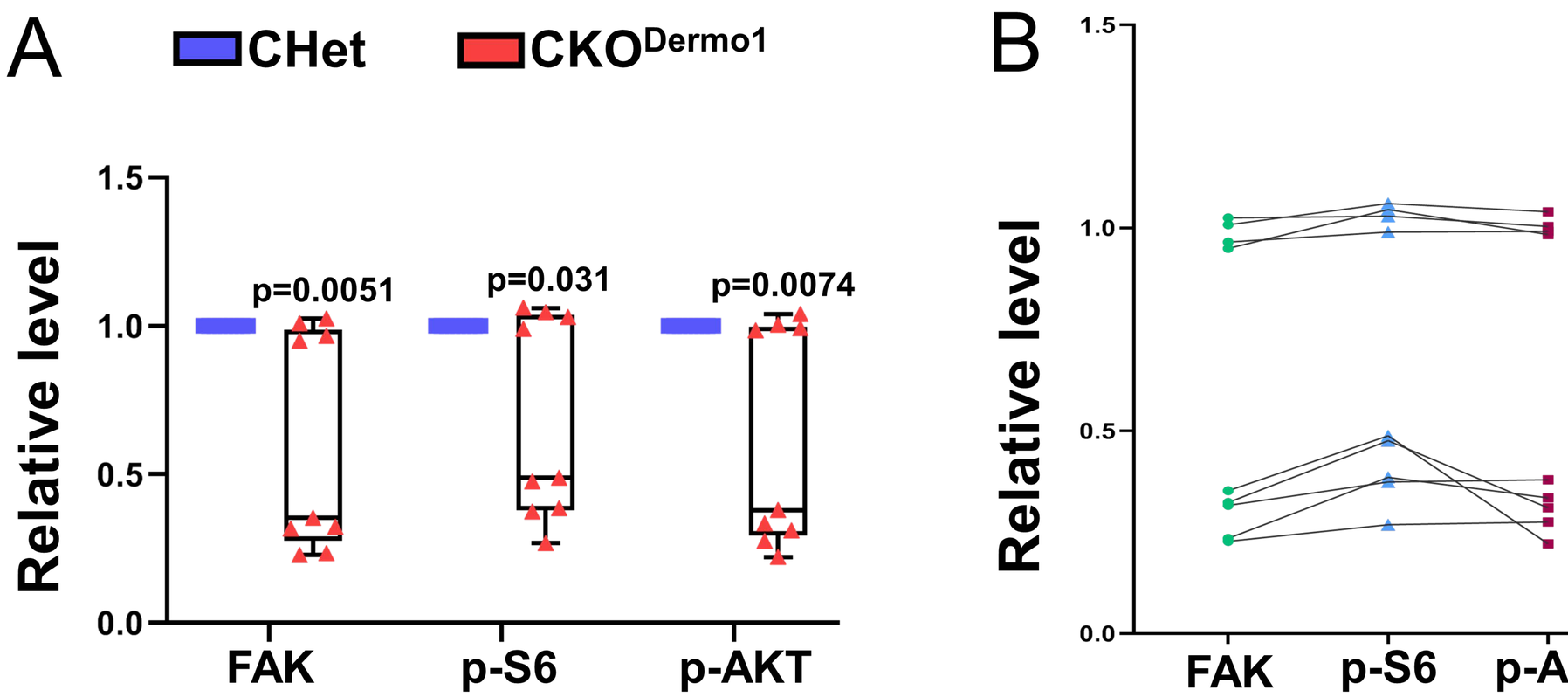

Figure S11. *Fak* deletion efficiency correlates with the decrease of phospho-S6 and phospho-AKT level. BMSCs isolated from CHet and CKO^{Dermo1} mice were analyzed by western blot on the protein level of FAK, phospho-S6 **(**p-S6), and phospho-AKT (p-AKT) in 9 independent experiments. (A) The relative protein levels of FAK, p-S6, and p-AKT were quantified by first normalizing to vinculin and then normalizing to CHet sample in each experiment. (B) The correlation between relative FAK level and the level of p-S6 and p-AKT in CKO^{Dermo1} BMSCs in each experiment. Round green dots indicate the FAK level of CKO^{Dermo1} relative to CHet, blue triangle indicates the p-S6 level of CKO^{Dermo1} relative to CHet, and red square indicates the p-AKT level of CKO^{Dermo1} relative to CHet; each line connects the dot, triangle, and square of the same experiment (n=9).

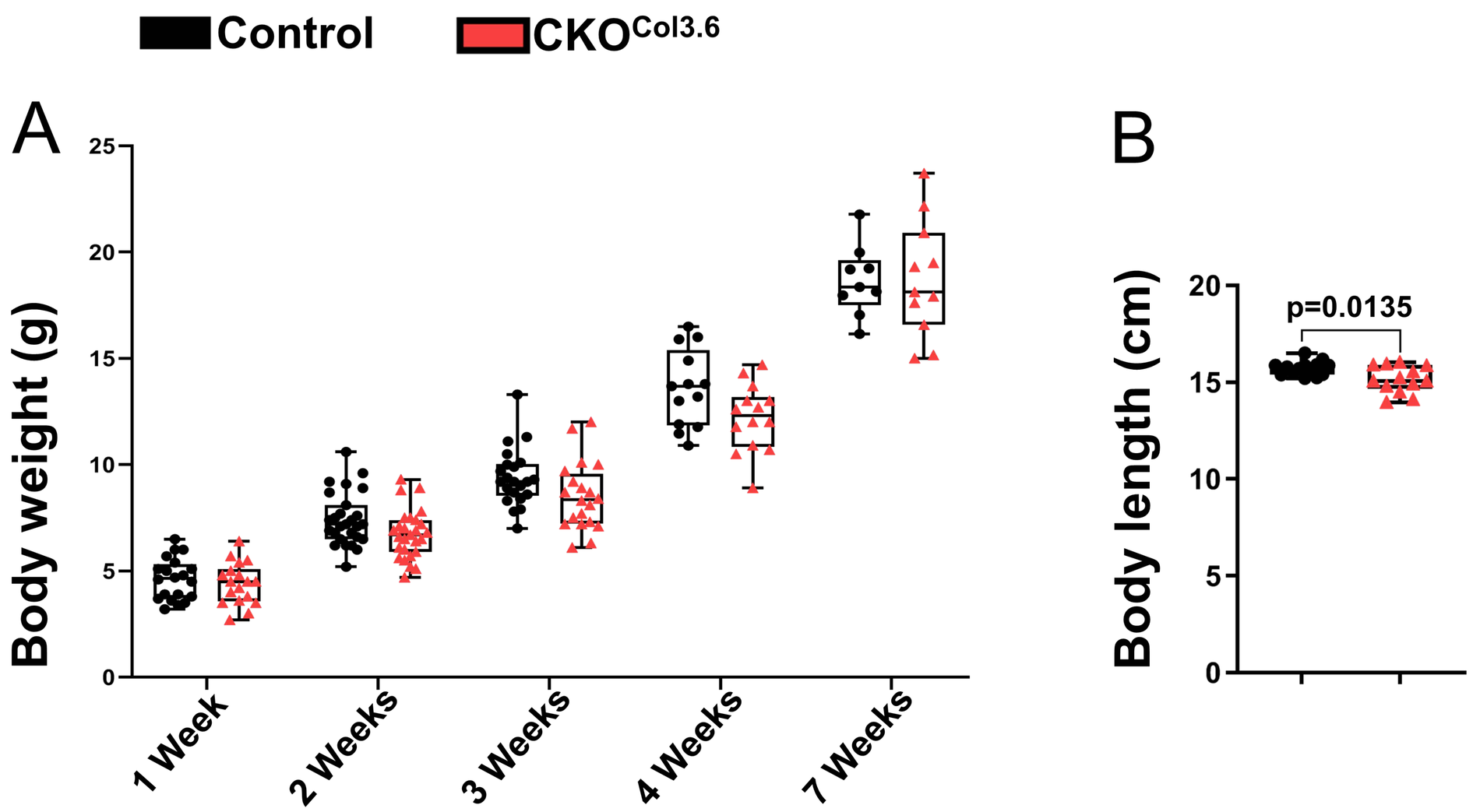

Figure S12. Body weight and body length of the *Fak*$^{flox/flox}$ (Control) and *Fak*$^{flox/flox}$;*Col3.6-Cre* (CKO$^{Col3.6}$) female mice. (A) Body weight of female control and CKO$^{Col3.6}$ mice at indicated ages (n=20, 27, 22, 13, 9 in 1 week, 2 weeks, 3 weeks, 4 weeks and 7 weeks respectively for control group; n=18, 27, 20, 14, 11 in week, 2 weeks, 3 weeks, 4 weeks and 7 weeks for CKO$^{Col3.6}$ group). (B) Body length of 7-week-old female control and CKO$^{Col3.6}$ mice (n=14 for control group and n=13 for CKO$^{Col3.6}$ group). Values were presented as median and interquartile range.

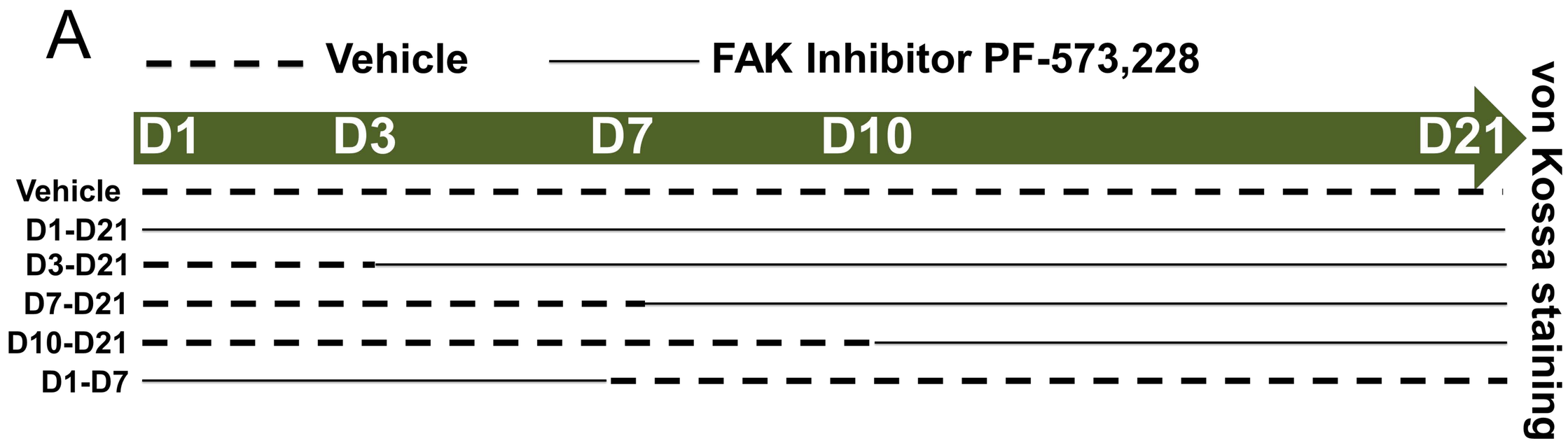

Figure S13. The effect of FAK kinase inhibition on BMSC osteogenic differentiation is cell differentiation stage-dependent. (A) Cartoon showing the experimental design of FAK inhibitor PF-573,228 treatment used in (B). Dashed line indicates vehicle treatment and solid line indicates 1 μM FAK inhibitor PF-573,228 treatment at indicated culture time in different groups: D1-D21 means inhibitor was added from day 1 to day 21; D3-D21 means inhibitor was added from day 3 to day 21; D7-D21 means inhibitor was added from day 7 to day 21; D10-D21 means inhibitor was added from day 10 to day 21; D1-D7 means inhibitor was added from day 1 to day 7. Von Kossa staining was performed at the end of 21 days culture for all groups. (B) Representative image of von Kossa staining in BMSCs treated with vehicle or FAK inhibitor at day 21 in different groups as described in (A). (C) Quantification of the mineralized nodule number in von Kossa staining as shown in (B). Each data point represents the average of one independent experiment (n=5 per group). Values were presented as median and interquartile range.

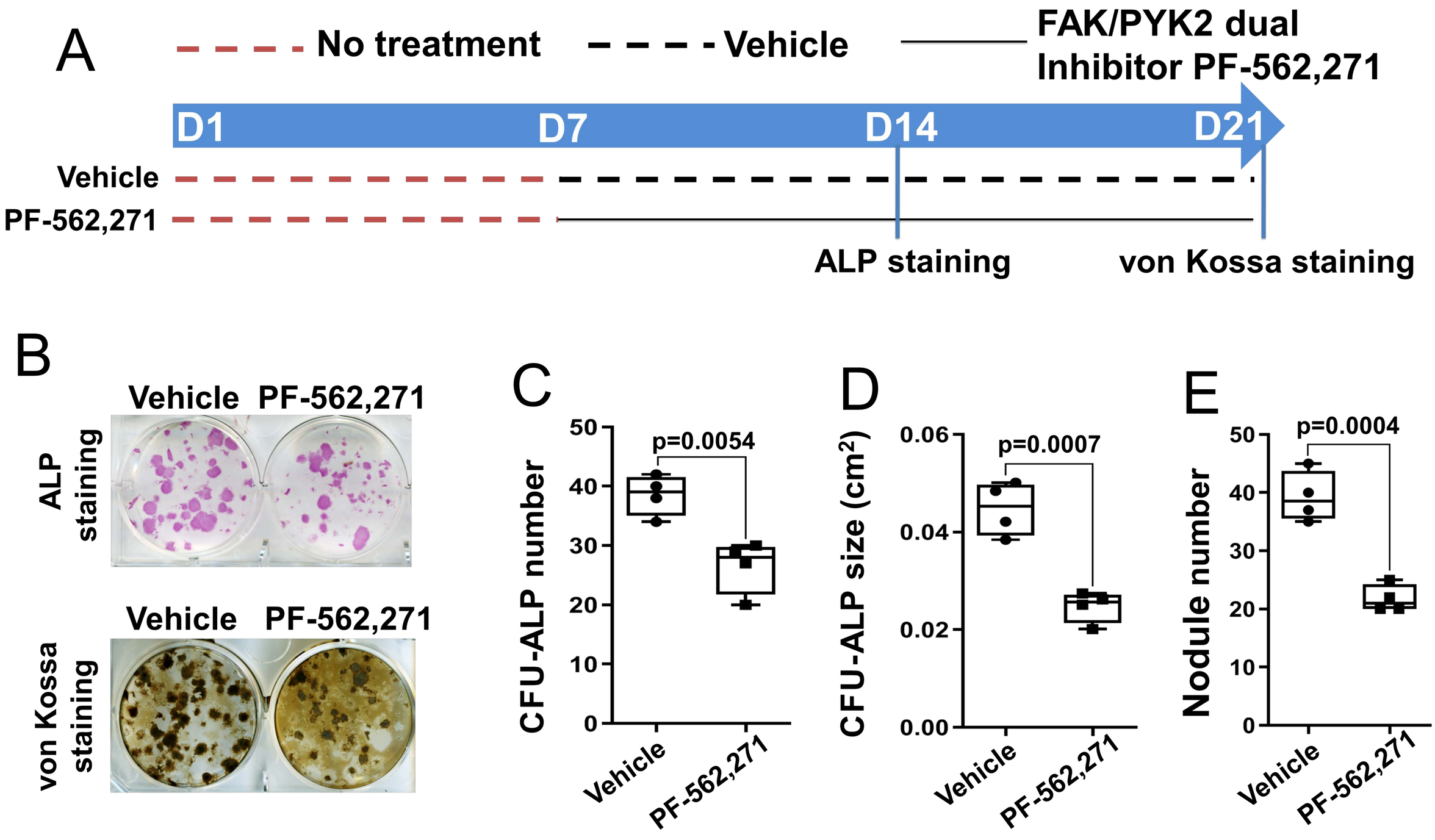

Figure S14. The effect of dual inhibition of FAK kinase and PYK2 kinase at later culture on the BMSC osteogenic differentiation. (A) Cartoon showing the experimental design of FAK/PYK2 dual inhibitor PF-562,271 treatment used in (B). Dashed red line represented no treatment, dashed black line represented vehicle treatment and solid black line represented 1 μM FAK/PYK2 dual inhibitor PF-562,271 treatment from day 7 to day 21. ALP staining and von Kossa staining were performed at day 14 and day 21 respectively. (B) Representative image of the ALP staining and von Kossa staining performed at day 14 and day 21 respectively as illustrated in (A). (C) Quantification of CFU-ALP number. (D) Quantification of CFU-ALP size. (E) Quantification of nodule number. Each data point represents the average of one independent experiment (n=4). Values were presented as median and interquartile range.

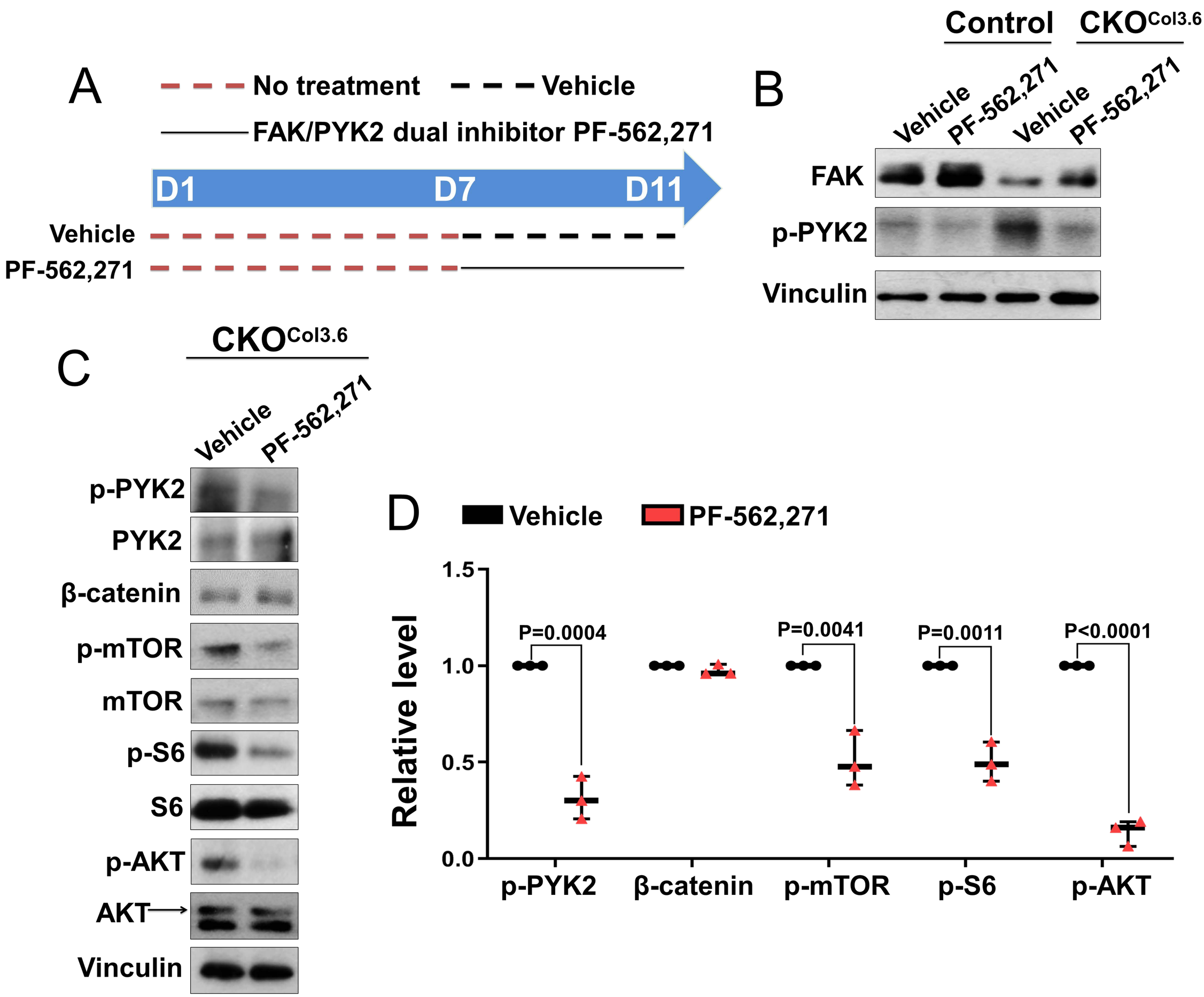

Figure S15. Dual inhibition of FAK kinase and PYK2 kinase decreases mTORC1 signaling in BMSCs isolated from *Fak*$^{flox/flox}$;*Col3.6-Cre* (CKO$^{Col3.6}$) mice. (A) Cartoon showing the experimental design of FAK/PYK2 dual inhibitor PF-562,271 treatment used in (B-D). Dashed red line indicates no treatment, dashed black line indicates vehicle treatment and solid black line indicates 1 μM PF-562,271 treatment. (B-C) BMSCs were isolated from *Fak*$^{flox/flox}$ (Control) and *Fak*$^{flox/flox}$;*Col3.6-Cre* (CKO$^{Col3.6}$) mice and the protein lysates were collected at day 11 culture; western blotting was performed using indicated antibodies. (D) Quantification of the relative protein levels illustrated in (C). Phospho-proteins were normalized to the respective total proteins and β-catenin was normalized to Vinculin (n=3). Values were presented as median and interquartile range.

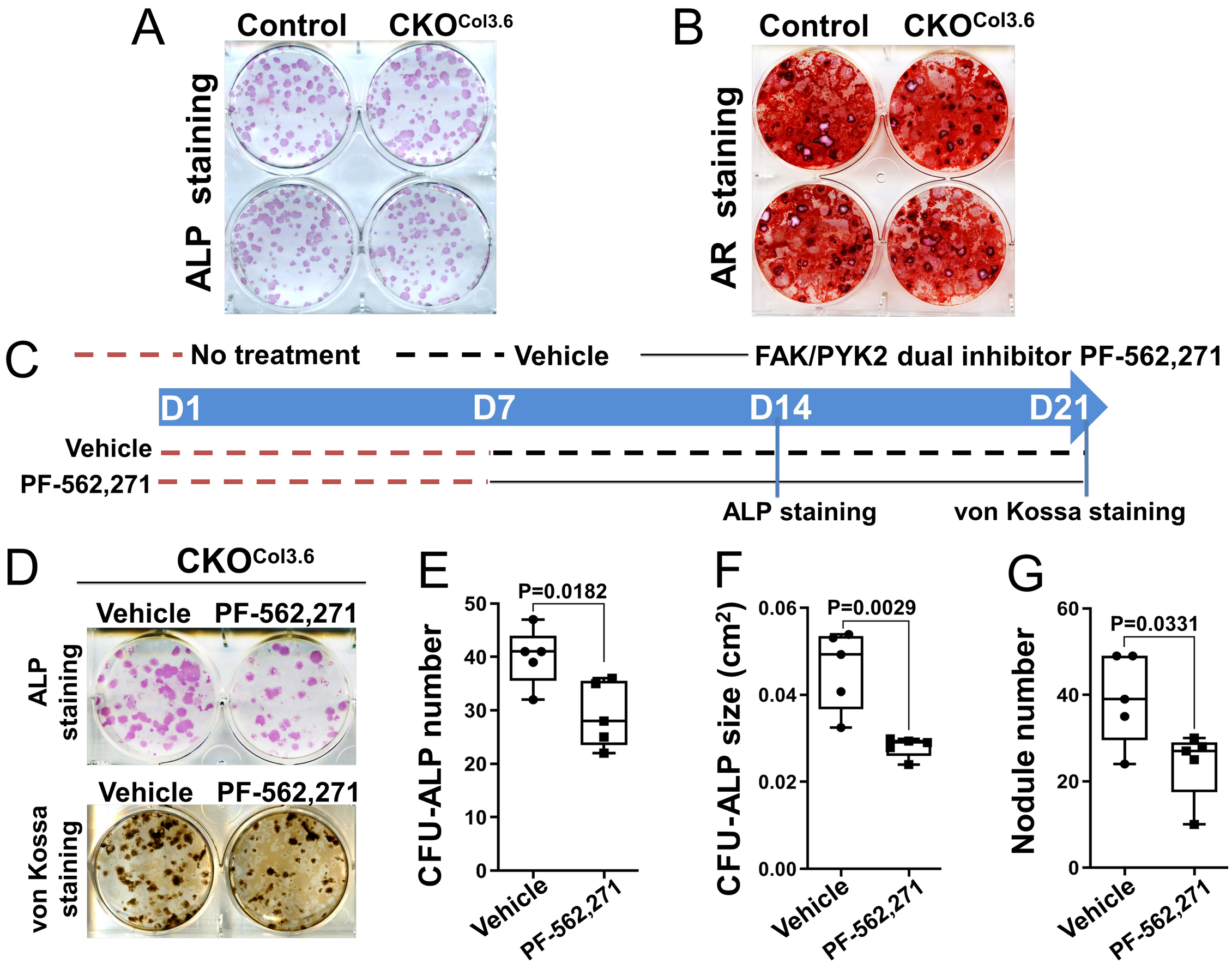

Figure S16. FAK/PYK2 dual inhibitor PF-562,271 inhibits osteogenic differentiation of BMSCs isolated from *Fak*$^{flox/flox}$;*Col3.6-Cre* (CKO$^{Col3.6}$) mice. (A-B) BMSCs were isolated from *Fak*$^{flox/flox}$ (Control) and *Fak*$^{flox/flox}$;*Col3.6-Cre* (CKO$^{Col3.6}$) mice and cultured in osteogenic medium: (A) Representative image of the ALP staining at day 10; (B) Representative image of the AR staining at day 21 (n=3). (C) Cartoon showing the experimental design of FAK/PYK2 dual inhibitor PF-562,271 treatment used in (D-G). Dashed red line represented no treatment, dashed black line represented vehicle treatment and solid black line represented 1 μM FAK/PYK2 dual inhibitor PF-562,271 treatment from day 7 to day 21. ALP staining and von Kossa staining were performed at day 14 and day 21 respectively. (D) Representative image of the ALP staining and von Kossa staining described in (C). (E) Quantification of CFU-ALP number. (F) Quantification of CFU-ALP size. (G) Quantification of nodule number. Each data point represents the average of one independent experiment (n=5). Values were presented as median and interquartile range.